Mechanisms for the stability of Al and B adatoms on the Si(111) $\sqrt{3}\times\sqrt{3}R30°$ surface

Sanwu Wang, M. W. Radny, and P. V. Smith*
Department of Physics, The University of Newcastle, Callaghan 2308, Australia
(Received 15 September 1998)

The bonding of aluminium and boron adatoms on the Si(111)$\sqrt{3}\times\sqrt{3}R30°$ surface has been investigated using *ab initio* density-functional theory methods in order to understand the difference in stability between different adatom bonding configurations. It has been found that the greater stability of the T_4 configurations compared to the H_3 geometries is mainly due to stronger covalent bonding between the adatom and the substrate in the T_4 structures. The difference in stability between the T_4 and S_5 topologies, on the other hand, is determined predominantly by charge redistribution. [S0163-1829(99)08503-3]

Si(111) surfaces chemisorbed by group-III elements have been widely studied as prototype metal-semiconductor systems.[1] At a coverage of one third of a monolayer, chemisorption of the group-III elements on a Si(111) surface leads to the formation of $\sqrt{3}\times\sqrt{3}R30°$ structures.[1] Being trivalent, each group-III atom is expected to saturate three silicon dangling bonds on the (111) surface. The threefold-coordinated adatom positions on the Si(111)$\sqrt{3}\times\sqrt{3}R30°$ surface are referred to as the T_4 and H_3 sites. The T_4 site lies directly above a second-layer silicon atom, while the H_3 site is above a fourth-layer Si atom. Periodic slab calculations have shown that the T_4 structures are lower in energy than the corresponding H_3 structures for the Si(111)$\sqrt{3}\times\sqrt{3}R30°$-Al, -Ga, and -In surfaces and good agreement between experiment and theory for the T_4 geometries has been achieved.[1–3] The most stable structure on the Si(111)$\sqrt{3}\times\sqrt{3}R30°$-B surface, on the other hand, has been found to be the so-called B-S_5 geometry where the boron atom substitutes for a second-layer silicon atom directly below the T_4 site, and the T_4 site is occupied by a silicon atom.[1,4]

While the preferred bonding sites of the group-III atoms have been well established, the question of why Al, Ga, and In prefer to bond at the T_4 sites, and B atoms at the S_5 sites, has not yet been answered satisfactorily. Only some conjectures have been made with respect to this issue. Over and Tong[5] suggested that the greater stability of the T_4 geometry compared to the H_3 geometry is due primarily to resonant bonding between the adatom and the Si atom directly below it. Nicholls, Reihl, and Northrup,[3] on the other hand, suggested that the lower total energy of the T_4 geometry is achieved by buckling of the second-layer silicon atoms, which may result in a larger overlap between the adatoms and the first-layer Si atoms in the T_4 topology than in the H_3 topology. For the boron case, several authors have suggested that relief of surface strain is the main reason for the stability of the B-S_5 geometry.[4] However, Wong *et al.* have argued that the B-S_5 geometry may introduce more strain into the silicon lattice than the B-T_4 geometry.[6] Charge transfer from the silicon adatom at the T_4 site to the substitutional S_5 boron atom was also considered to play a role in stabilizing the B-S_5 structure.[4] To our knowledge, none of the above conjectures have yet been verified by any quantitative data.

In the present work, we perform *ab initio* density-functional theory (DFT) cluster calculations for the Si(111)$\sqrt{3}\times\sqrt{3}R30°$-Al and -B surfaces. Quantitative data for explaining the difference in stability between different geometries has been obtained. Two mechanisms have been introduced to explain the origin of the preferred bonding sites. While a difference in covalent bonding has been found to be the main reason for the difference in stability between the T_4 and H_3 geometries, a difference in the Coulomb interaction has been proposed to be responsible for the difference in stability between the T_4 and S_5 geometries.

The T_4 and H_3 adatom bonding configurations have been simulated by the clusters Al(B)$Si_{14}H_{27}$ and Al(B)$Si_{16}H_{25}$, shown in Figs. 1(a) and 1(b), respectively. The Al(B)-S_5 configuration is represented by the same cluster as the T_4 configuration only with the adatom being a silicon atom and the second-layer atom directly below the adatom being an Al(B) atom. The equilibrium geometries of the clusters were determined by minimizing the total energy of each cluster with respect to the coordinates of the adatom and its six nearest-neighbor Si atoms (for the H_3 topologies), or with respect to its four nearest neighbors and the underlying third-layer Si atom (for the T_4 and S_5 geometries). The all-electron *ab initio* DFT method at the B3LYP level has been employed in all of the calculations. The B3LYP option represents a hybrid method for exchange and correlation that incorporates an exact HF exchange energy functional, and a semiempirical combination of a local and nonlocal spin-density electron correlation functional.[7,8] The moderately sophisticated double-ζ basis set 6-31$G(d)$,[8] which includes one set of d polarization functions for the heavy atoms, has been used to obtain the minimum-energy configuration and the adatom binding energy for each cluster. Mulliken charge population analyses, and molecular orbital overlap population (MOOP) curves, have been used to analyze the electronic structure of each cluster. The MOOP function measures the bonding or antibonding character of the interaction between two orbitals weighted by their overlap population.[9] The integral of the MOOP function up to the highest occupied molecular orbital (HOMO) gives a measure of the net bonding (antibonding) character of a particular pair of orbitals. The set of δ-function peaks yielded by our finite cluster calculations are artificially broadened by a Lorentzian of width 0.1 eV in order to yield continuous functions. In a separate study we have found that the use of STO-nG and

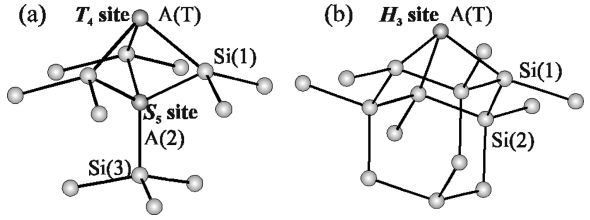

FIG. 1. The clusters used to simulate the adatom bonding configurations on the Si(111)$\sqrt{3}\times\sqrt{3}R30°$ surface, (a) Al(B)$Si_{14}H_{27}$ for the T_4 and S_5 topologies; (b) Al(B)$Si_{16}H_{25}$ for the H_3 geometries. The hydrogen atoms that have been used to saturate the bulk dangling bonds are not shown. The adatom, its first-, second- and third-layer nearest-neighbor silicon atoms, and the second layer atom in the S_5 site are denoted by $A(T)$, Si(1), Si(2), Si(3), and $A(2)$, respectively.

STO-$nG(d)$ basis functions[8] can produce reasonable Mulliken populations and MOOP curves for silicon systems.[10] We have therefore chosen to use the STO-$6G(d)$ basis set[8] in all of our calculations of the Mulliken charge and MOOP distribution functions.

The calculated results for the optimized geometries and the adatom binding energies are presented in Table I. Compared with the H_3 geometries, the T_4 topologies exhibit much larger downward displacements of the second and the third-layer silicon atoms. The movement of the first-layer silicon atoms along the (111) plane is also significantly larger in the T_4 geometries than in the H_3 topologies. The main difference between the Al-T_4 and Al-S_5 geometries is the larger downward displacement of all of the first three-layer atoms in the Al-S_5 topology. Movements of the first-layer silicon atom in the B-S_5 geometry is seen to be much larger than in the B-T_4 topology, while the second and third-layer atoms show less movement in the B-S_5 geometry than in the B-T_4 geometry, with the third-layer silicon atom in the B-S_5 geometry remaining essentially at the bulk position. The only currently available experimental data for the binding energies of the adatoms is for the Al-T_4 structure. The desorption energy of the Al adatom on the Si(111)$\sqrt{3}\times\sqrt{3}R30°$-Al surface has been estimated to be 3.8 eV.[11] Our calculated binding energy of 3.73 eV for the Al adatom at the T_4 site is in excellent agreement with this experimental result. The total energy of the Al-S_5 cluster has been determined to be 1.55 eV higher than that of the Al-T_4 cluster. The total energy of the B-S_5 cluster, on the other hand, has been found to be 1.75 eV lower than the B-T_4 cluster. We can thus conclude that the B-S_5 and Al-T_4 geometries are more stable than the B-T_4 and Al-S_5 topologies, respectively. The T_4 and H_3 clusters include different numbers of the atoms, and hence we cannot use the total-energy difference to determine the preferred adatom bonding sites. However, using the adatom binding energies as a measure of the relative stability of the T_4 and H_3 geometries suggests that the T_4 topologies are more stable than the corresponding H_3 geometries. Combining all of the above results leads us to conclude that the Al-T_4 and B-S_5 structures are the most stable configurations on the Si(111)$\sqrt{3}\times\sqrt{3}$-Al and Si(111)$\sqrt{3}\times\sqrt{3}$-B surfaces, respectively. This is in agreement with the experimental data and previous theoretical results.[1]

TABLE I. The interatomic distances (in Å), the substrate-atom displacements from their ideal positions (in Å), and the binding energies (BE) of the adatoms (in eV), for the T_4, H_3, and S_5 geometries. The direction of the z axis, the threefold symmetry axis of each of the clusters, is that of the surface normal, which is perpendicular to the (111) plane. The r coordinate is the perpendicular distance to the z axis.

	Si(111)-Al			Si(111)-B		
	T_4	H_3	S_5	T_4	H_3	S_5
$d_{A(T)\text{-Si}(1)}$	2.56	2.57	2.49	2.15	2.28	2.40
$r_{A(T)\text{-Si}(1)}$	2.12	2.18	2.13	2.00	2.06	1.95
$d_{A(T)\text{-}A(2)}$	2.51	3.15	2.43	2.05	2.91	2.20
$\Delta r_{\text{Si}(1)}$	−0.10	−0.04	−0.08	−0.22	−0.16	−0.27
$\Delta z_{\text{Si}(1)}$	−0.02	0.03	−0.07	−0.04	0.03	−0.31
$\Delta z_{\text{Si}(2)}$	−0.31	−0.04	−0.43	−0.53	−0.07	−0.32
$\Delta z_{\text{Si}(3)}$	−0.20	0.01	−0.35	−0.36	0.03	0.01
BE	3.73	3.53	4.33	4.68	3.46	5.33

TABLE II. The integrated MOOP function for bonds between pairs of surface atoms.

	Si(111)-Al			Si(111)-B		
	T_4	H_3	S_5	T_4	H_3	S_5
$A(T)$-Si(1)	0.47	0.43	0.56	0.70	0.54	0.59
$A(T)$-$A(2)$	0.14	0.01	0.22	0.37	−0.01	0.22
Si(1)-$A(2)$	0.65	0.69	0.54	0.58	0.71	0.69
Si(1)-Si(1)	−0.02	−0.02	−0.02	−0.02	−0.03	−0.02
$A(2)$-Si(3)	0.78	0.77	0.70	0.85	0.81	0.80

Table II presents values of the integrated MOOP function for the different surface bonds. These values provide us with an estimate of the bond strength between pairs of atoms within each cluster. The overlap population of the bond between the Al or B adatom and one of the first-layer silicon atoms in the T_4 geometry [denoted as $A(T)$-Si(1) with $A(T)$ being the Al, B, or Si adatom) has been calculated to be 0.47 (Al-T_4) or 0.70 (B-T_4), whereas the corresponding bond in the H_3 topology has overlap population of 0.43 (Al-H_3) or 0.54 (B-H_3). This suggests that the $A(T)$-Si(1) bond is stronger in the T_4 structure than in the H_3 geometry. Compared with the B-H_3 topology, the significantly shorter component of the B-Si(1) bond along the (111) plane, and the significantly shorter overall B-Si(1) bondlength, produces larger overlap between the B adatom and its nearest first-layer atoms in the B-T_4 structure than for the H_3 structure. The stronger bonding in the Al-T_4 geometry mainly originates from the shorter component of the Al-Si(1) bond along the (111) plane, which increases the overlap between the $3p_{xy}$ orbital of the Al adatom and the $3p_z$ orbitals of the first-layer silicon atoms.

The interaction between the adatom and its underlying second-layer silicon atom in the T_4 geometry [hereafter referred to as $A(T)$-Si(2)] has a net bonding character. However, this bond is much weaker than the $A(T)$-Si(1) bond as the overlap population is significantly smaller (0.14 vs 0.47 for the Al case, 0.37 vs 0.70 for the B case). The $A(T)$-Si(2) bond in the H_3 topology is close to nonbonding with an

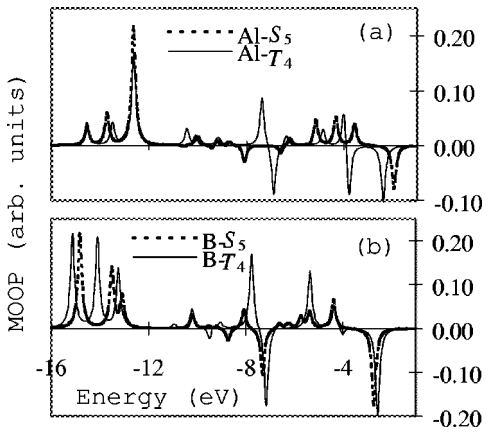

FIG. 2. MOOP distribution functions of the $A(T)$-Si(2) bonds.

overlap population of almost zero. The $A(T)$-Si(2) distances in the T_4 geometries are slightly smaller than the corresponding $A(T)$-Si(1) bondlengths. The prediction of much weaker $A(T)$-Si(2) bonding is thus somewhat surprising. The MOOP curves for the $A(T)$-Si(2) bonds shown in Fig. 2, however, show that unlike the $A(T)$-Si(1) bonds for which bonding character has been found to be predominant among all of the molecular orbitals, there are significant antibonding contributions to the $A(T)$-Si(2) bonds. These antibonding contributions partly cancel the bonding contributions, and result in an overall weakening of the $A(T)$-Si(2) bonds. The possible origin of this antibonding can be seen by considering just a single molecular orbital. Figure 3 shows the HOMO charge distribution for the Al-T_4 geometry. The main contributions of the adatom and the second-layer silicon atom to this molecular orbital come from the $3p_{xy}$ orbitals. We observe that there is no bonding overlap between these two orbitals but rather an antibonding contribution due to the sign of the $3p_{xy}$ orbital of the Al adatom being everywhere opposite to that of the underlying second layer atom. This is in agreement with the MOOP curve in Fig. 2(a) where an antibonding contribution to the Al-Si(2) bond from the HOMO is clearly seen.

Table II reveals that overlap between the first- and second-layer atoms is less for the T_4 structures than for the H_3 geometries. However, the larger overlap of the adatom and the first-layer silicon atoms, and bonding between the adatom and the second-layer silicon atom directly below it, more than compensates for this effect in the T_4 structures and results in greater stability of the T_4 topologies than the corresponding H_3 topologies.

The Si(1)-Si(2) bonds in the Al-T_4 geometry are stronger than the Si(A)-Si(1) bonds in the Al-S_5 geometry (with overlap population of 0.65 vs 0.56). However, this effect would appear to be largely cancelled by the larger overlap between the Al atom and the first-layer silicon atoms in the Al-S_5 geometry than in the Al-T_4 topology (0.54 vs 0.47). The overall picture suggested by the covalent bonding, therefore, is that the Al-T_4 and Al-S_5 topologies may be nearly equal in stability. This, however, is in contrast to the total-energy calculations. A similar situation occurs for the B case. The bonding between the boron atom and the first-layer silicon atoms in both the T_4 and S_5 geometries is of similar magnitude (0.70 vs 0.69). The strength of the Si(1)-Si(2) bonds in the B-T_4 geometry (0.58), and the Si(A)-Si(1) bonds in the B-S_5 geometry (0.59), are almost the same. However, the overlap between the B adatom and the second-layer atom in the B-T_4 structure (0.37) is obviously larger than the corresponding bond in the B-S_5 geometry (0.22). The overall covalent bonding in the B-T_4 geometry thus seems somewhat stronger than that in the B-S_5 geometry.

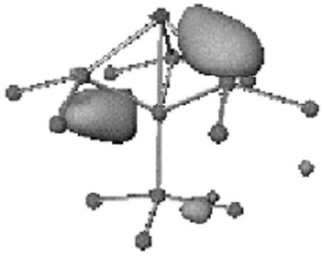

FIG. 3. Charge distributions of the HOMO in the Al-T_4 configuration.

TABLE III. Mulliken charge for the surface atoms, and the Coulomb potential energies E_c (in units of eV), for the T_4, H_3, and S_5 geometries.

	Si(111)-Al			Si(111)-B		
	T_4	H_3	S_5	T_4	H_3	S_5
$A(T)$	0.366	0.415	0.073	−0.183	−0.089	0.064
Si(1)	−0.083	−0.093	−0.091	0.031	0.012	0.064
$A(2)$	−0.091	−0.035	0.206	−0.07	−0.012	−0.375
Si(3)	0.021	−0.002	−0.043	0.034	−0.004	0.099
E_c	−0.50	−0.58	−0.21	−0.08	−0.01	−0.69

In the above discussions, we have not considered the possible effects of ionic bonding. The interaction of an Al or B atom with the silicon surface may result in charge transfer so that a purely covalent description of the bonding may not be sufficient. In Table III we have presented data derived from a Mulliken charge population analysis of our various clusters. The general picture is that some charge is transferred from the Al atom to its neighboring silicon atoms, while the boron atom always acquires some charge. The actual amount of charge transfer, however, differs from geometry to geometry. A rough estimation of the difference in ionic bonding between the T_4, H_3, and S_5 configurations can be obtained by calculating the Coulomb potential energies using the Mulliken charge populations. These values are given in Table III. Only interactions between the adatom and its close neighbors have been considered as the charge on more distant atoms are almost the same as the bulk value. The differences in Coulomb potential energy between the Al-T_4 and Al-H_3 geometries, and between the B-T_4 and B-H_3 topologies, are so small that we can safely conclude that ionic bonding does not significantly contribute to the difference in stability between the T_4 and H_3 geometries. The above covalent model should thus be sufficient to explain the difference in stability between these two competing geometries.

In the Al-T_4 geometry the Al adatom transfers charge to its four nearest-neighboring silicon atoms. This results in an attractive Coulomb force between the adatom and its neighbors. In the Al-S_5 topology, both the Si adatom and the Al atom, which is now at the S_5 site, transfer some charge to

other atoms. This produces a substantial electrostatic repulsion between the silicon adatom and the subsurface Al atom and results in the Coulomb energy for the Al-S_5 cluster being 0.29 eV higher than for the Al-T_4 cluster. The ionic model thus predicts the Al-T_4 geometry to be more stable than the Al-S_5 topology. In the B-S_5 geometry, the boron atom obtains a significant charge from its five nearest-neighbor silicon atoms and thus forms five attractive bonds. Both the B adatom and the underlying second-layer silicon atom in the B-T_4 topology obtain charge, which results in a Coulomb repulsion between them. The boron adatom at the T_4 site does give rise to attractive interactions with its three nearest first-layer silicon atoms but these are less significant than the corresponding forces in the B-S_5 geometry because the amount of the charge transfer in the B-S_5 geometry is much larger than in the B-T_4 topology. Summing all of the contributions, the Coulomb energy of the B-S_5 topology is estimated to be 0.61 eV lower than the B-T_4 geometry. This ionic model is thus consistent with the total-energy calculations in predicting that the B-S_5 geometry will be more stable than the B-T_4 geometry.

In conclusion, we have investigated the bonding characteristics of three different bonding configurations of Al and B atoms on the cluster modeled Si(111)$\sqrt{3}\times\sqrt{3}R30°$ surface. We have shown that while a model based solely on considerations of covalent bonding provides an adequate explanation for the greater stability of the T_4 structures over the corresponding H_3 geometries, an ionic bonding model is needed to show the difference in stability between the T_4 and S_5 geometries.

S. Wang would like to thank the Australian Government and the University of Newcastle for financial support. We would also like to acknowledge the Supercomputer Facility of the Australian National University for the provision of computing time during the course of this work.

*Author to whom correspondence should be sent. Electronic address: phpvs@cc.newcastle.edu.au

[1] J. P. LaFemina, Surf. Sci. Rep. **16**, 133 (1992); W. Mönch, *Semiconductor Surfaces and Interfaces*, Springer Series in Surface Sciences 26 (Springer-Verlag, Berlin, 1993); H. N. Waltenburg and J. T. Yates, Jr., Chem. Rev. **95**, 1589 (1995).

[2] J. E. Northrup, Phys. Rev. Lett. **53**, 683 (1984); J. M. Nicholls, P. Mårtensson, G. V. Hansson, and J. E. Northrup, Phys. Rev. B **32**, 1333 (1985).

[3] J. M. Nicholls, B. Reihl, and J. E. Northrup, Phys. Rev. B **35**, 4137 (1987).

[4] R. L. Headrick, I. K. Robinson, E. Vlieg, and L. C. Feldman, Phys. Rev. Lett. **63**, 1253 (1989); P. Bedrossian, R. D. Meade, K. Mortensen, D. M. Chen, J. A. Golovchenko, and D. Vanderbilt, *ibid.* **63**, 1257 (1989); I.-W. Lyo, E. Kaxiras, and Ph. Avouris, *ibid.* **63**, 1261 (1989).

[5] H. Over and S. Y. Tong, in *Physical Structure*, edited by W. N. Unertl, *Handbook of Surface Science* (Elsevier Science, New York, 1996), Vol. 1.

[6] Y.-T. Wong, B. Schubert, and R. Hoffmann, J. Am. Chem. Soc. **114**, 2367 (1992).

[7] A. D. Becke, J. Chem. Phys. **98**, 5648 (1993); S. H. Vosko, L. Wilk, and M. Nusair, Can. J. Phys. **58**, 1200 (1980); C. Lee, W. Yang, and R. G. Parr, Phys. Rev. B **37**, 785 (1988).

[8] M. J. Frisch *et al.*, GAUSSIAN 94 (Revision E.2), Gaussian Inc., Pittsburgh, PA, 1995.

[9] R. Hoffmann, *Solids and Surfaces: A Chemist's View of Bonding in Extended Structures* (VCH, New York, 1988).

[10] S. Wang, M. W. Radny, and P. V. Smith (unpublished).

[11] A. A. Saranin, E. A. Khramtsova, and V. G. Lifshits, Surf. Sci. **302**, 57 (1994).